

# Study on the intermolecular interactions between the functional moieties in ferrocene-terminated alkanethiol self-assembled monolayer on gold

Yan Guo, Jianwei Zhao\*, Junjie Zhu

Key Laboratory of Analytical Chemistry for Life Science, School of Chemistry and Chemical Engineering, Nanjing University, 210093, Nanjing, PR China

Received 27 May 2007; received in revised form 7 December 2007; accepted 7 December 2007

Available online 16 January 2008

## Abstract

In this paper, we used two kinds of ionic surfactants, sodium dodecylbenzene sulfonate and cetyltrimethylammonium bromide, to explore how the intermolecular interaction affected the electrochemical behavior of 11-Ferrocenylundecanethiol (HSC<sub>11</sub>Fc) self-assembled monolayers (SAM). While HSC<sub>11</sub>Fc was mixed with octanethiol in a low mole ratio, we found a well-defined redox wave. After the treatment with both surfactants, a shoulder peak more positive to the main wave emerged. This observation was explained with the variation of the local microenvironment as evidenced by the reorganization energy. Without the surfactant interaction, the pure HSC<sub>11</sub>Fc SAM also exhibited the similar shoulder peak, which can be further enhanced by the treatment with the surfactants. By gradually changing the surface coverage of ferrocene moiety, it proved that the shoulder peak was originated from the intermolecular interaction by either the ionized surfactant or the neighboring ferrocenium ions.

© 2007 Elsevier B.V. All rights reserved.

**Keywords:** Self-assembled monolayer; Ferrocene-terminated alkanethiol; Surfactant; Microenvironment; Surface electrochemistry

## 1. Introduction

Since the pioneering work by Nuzzo and Allara in 1983 [1], self-assembled monolayers (SAMs) of alkanethiols have gained much attention in the interfacial electrochemistry and other research fields [2,3]. Due to the stable Au–S chemisorption, the functionalized self-assembled alkanethiols have been used widely to anchor the electroactive species onto electrodes, presenting a model system for studying the interfacial electron transfer process and the interaction between the immobilized functional moieties [4–19].

Ferrocene-terminated alkanethiol system, the most representative example of electroactive SAM, has been studied intensively. One limitation that makes the theoretical analysis of electron transfer kinetics more complicated is the peak distortion [6,9,17,18,20–26], though these observations can be intuitively assigned to the interaction between the redox centers in the dense ferrocene-terminated SAM [27,28].

An approach to overcome the problems arising from intermolecular interactions is to dilute the electroactive species in the monolayer by mixing alkanethiols [6,7,29]. Using this method, Chidsey et al. [6–8] and Creager et al. [12–16,29,30] have carried out preeminent work on the long-range electron transfer kinetics. Their studies also showed that the monolayer thickness and the terminal group affect the redox potential. In the succeeding studies, some mixed monolayers present nonideal electrochemical behavior such as peak-broadening, peak asymmetry or shoulder peak [6,12–14,19,21,23,31–38]. People considered many possible reasons to explain these phenomena. In particular, the peak broadening and the shoulder peak have been assigned to the aggregation of the electroactive species [6,11]. Several other effects such as different structural order of the monolayer [9], double-layer effects [11,13,14,31,32], nanoscale phase separation [24,33], neighboring ferrocenium ion effect [21,34], and inhomogeneity of the ferrocene moieties within the monolayer [35–38] have been considered as well.

Another consideration is based on the solvent polarization [39]. The nature and the concentration of anions in the electrolyte are evidenced to affect the position and the shape of the redox waves [9–12,18,26,40]. In order to form the

\* Corresponding author. Tel./fax: +86 25 83596523.

E-mail address: [Zhaojw@nju.edu.cn](mailto:Zhaojw@nju.edu.cn) (J. Zhao).

specifically polar microenvironment, one can use the  $\omega$ -substituted alkanethiols with polar functional groups. Reinhoudt et al. [35] and Lennox et al. [37] studied these systems, and found that the mixed monolayer with the alkanethiols functionalized by carboxylic acid and/or amine group may change the peak shapes. These results imply that the polar microenvironment plays the important roles in the electrochemical process.

Surfactants that have long hydrophobic tail and ionic head may form the microscopic polar environment and are used widely in the fundamental researches and technologies [41–44]. These amphiphilic molecules can adsorb strongly at solid/solution interfaces, forming a specific stable interface that may, then, influence the interfacial electrochemistry [45,46]. In this paper, we use two typical ionic surfactants as probes to study the intermolecular interactions between the electroactive Ferrocene (Fc) groups in the dilute and dense 11-ferrocenylundecanethiol (HSC<sub>11</sub>Fc) self-assembled monolayer on gold. Their influence on the electrochemical behavior is evidenced, and explained by using the local polar microenvironment.

## 2. Experimental details

### 2.1. Chemical

11-bromoundecanoic acid (Tokyo Chemical Industry Co., Ltd, Japan), ferrocene (Shanghai Chemical Reagent Co., Ltd, China), 1-octanethiol (HSC<sub>8</sub>) (Alfa Aesar), sodium dodecylbenzene sulfonate (SDBS) (Shanghai Lingfeng Chemical Reagent Co., Ltd, China), cetyltrimethylammomium bromide (CTAB) (Jiangsu Huakang Chemical Co., Ltd, China) are used as received. All other chemicals are of analytical grade without further purification. Water is purified via a Purelab Classic system with a resistance of 18.2 M $\Omega$  cm.

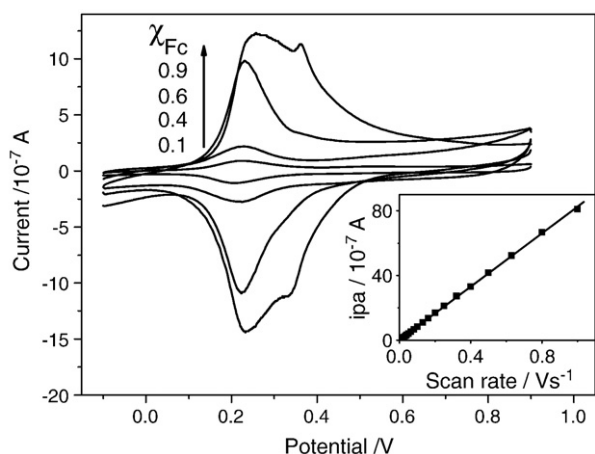


Fig. 1. Cyclic voltammograms of the mixed monolayers of HSC<sub>11</sub>Fc and HSC<sub>8</sub> in 0.1 M HClO<sub>4</sub> electrolyte. The total concentration of the mixed adsorption solution is 1 mM. The mole fractions ( $\chi_{Fc}$ ) of HSC<sub>11</sub>Fc in solution are 0.9, 0.6, 0.3 and 0.1, respectively. Scan rate: 0.1 V s<sup>-1</sup>. Reference electrode: SCE, counter electrode: Pt. Inset is the linear relation of peak currents versus various scan rates for the anodic process of  $\chi_{Fc}$  = 0.6.

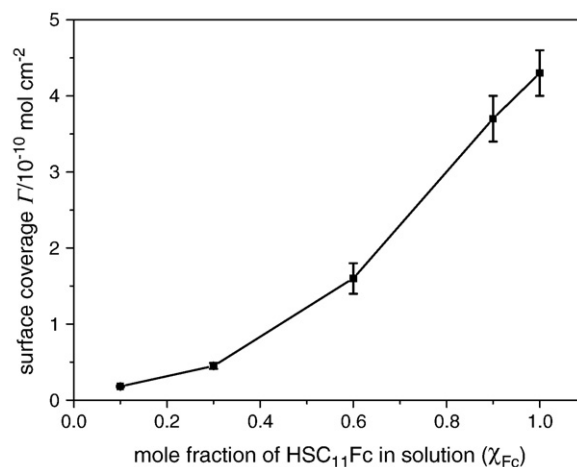


Fig. 2. Ferrocene surface coverage versus mole fraction ( $\chi_{Fc}$ ) of HSC<sub>11</sub>Fc in ethanol adsorption solution. The total concentration of the HSC<sub>11</sub>Fc and HSC<sub>8</sub> mixed adsorption solution is 1 mM.

### 2.2. Preparation of 11-ferrocenylundecanethiol

HSC<sub>11</sub>Fc is synthesized according to the literature [9]. In brief, ferrocene initially reacts with 11-bromoundecanoyl chloride which is converted by 11-bromoundecanoic acid and then is treated with zinc–mercury amalgum to lead to the formation of 11-bromoundecylferrocene. Then, 11-bromoundecylferrocene is refluxed for about 3 h in the presence of thiourea in ethanol solution and then refluxes for another 2 h with sodium hydroxide. Finally, the objective product is purified by column chromatography by using silica gel and characterized by <sup>1</sup>H Nuclear magnetic resonance (300 MHz, CDCl<sub>3</sub>) ( $\delta$ : 4.17 (br, 5H, C<sub>3</sub>H<sub>5</sub>\*), 3.92–4.05 (m, 4H, C<sub>5</sub>H<sub>4</sub>\*), 2.63 (t, 2H, CH<sub>2</sub>\*SH), 2.33 (t, 2H, FcCH<sub>2</sub>\*), 1.61–1.78 (m, 2H, CH<sub>2</sub>\*CH<sub>2</sub>SH), 1.41–1.58 (m, 2H, FcCH<sub>2</sub>CH<sub>2</sub>\*), 1.25–1.38 (m, 14H, CH<sub>2</sub>\*) ) and EI-MS (calc/found) (372/372).

### 2.3. Electrochemistry measurement

Electrochemistry experiments are performed on CHI 660B electrochemical workstation (Shanghai Chenhua Apparatus Corporation, China) and LK2005 electrochemical workstation (Tianjin Lanlike Chemistry & Electron High-Tech Co. Ltd., China). All experiments are carried out using a conventional three-electrode system with a polycrystalline gold disk electrode (2.0 mm diameter, CHI 101, CHI Instruments, USA) as the working electrode, a platinum wire as the auxiliary electrode, and a saturated calomel electrode (SCE) as the reference electrode. All potential values are given with respect to SCE.

The gold electrode is sequentially polished with 1.0, 0.3, and 0.05  $\mu$ m  $\alpha$ -Al<sub>2</sub>O<sub>3</sub> powder and rinsed thoroughly with pure water. Then the gold electrode is electrochemically cleaned by potential cycling in 0.1 M H<sub>2</sub>SO<sub>4</sub> in the potential range between –0.1 and 1.5 V until typical cyclic voltammogram of clean gold is obtained. The real surface area of the gold electrode is determined by the integration of the cathodic peak of cyclic voltammogram during the reduction of superficial AuO. The charge of 0.386 mC cm<sup>-2</sup> is accepted as the charge necessary to

Table 1

The full-width at half-maximum of the anodic voltammetric wave ( $\Delta E_{fwhm}$ ), the apparent formal potential ( $E^{\circ'}$ ) and the surface coverage ( $\Gamma$ ) of the mixed monolayer of HSC<sub>11</sub>Fc and HSC<sub>8</sub> with different ratio

$\chi_{Fc}$	$\Delta E_{fwhm}/mV$	$E^{\circ'}/mV$	$\Gamma/10^{-10} \text{ mol cm}^{-2}$
0.1	103	217	0.18±0.01
0.3	119	224	0.45±0.04
0.6	124	228	1.6±0.2
0.9	<sup>a</sup>	246 <sup>b</sup>	3.7±0.3

<sup>a</sup>There are two peaks too close to define the full-width at half-maximum of each voltammetric wave precisely.

<sup>b</sup> $E^{\circ'}$  of the first main peak.

form a monolayer of electrosorbed O in the form of AuO [47,48]. The roughness factor of Au electrodes is in the range between 1.5 and 1.8.

#### 2.4. Preparation of the modified gold electrodes

After rinsing with pure water and ethanol, the gold electrode is immersed in the HSC<sub>11</sub>Fc ethanol solution (~1 mM) or mixed thiol ethanol solution (the mixed HSC<sub>11</sub>Fc and alkanethiol solution with total concentration of 1 mM is sonicated for 2–3 min before self-assembly). Over more than 12 h dipping time, the modified electrode is drawn out from the solution and rinsed with copious amount of ethanol and pure water prior to transfer into electrochemical cell. As for the modulation of surfactants, the modified gold electrode is immersed in 0.05 M surfactant solution for 6 h and rinsed with copious amount of pure water before use. Electrolyte solutions are deoxygenated by purified nitrogen and a nitrogen atmosphere is maintained over the solutions during the experiments. All experiments have been carried out at 27±2 °C.

### 3. Results and discussion

#### 3.1. Mixed monolayer of ferrocene-terminated thiols and octanethiols

So far, most studies on electrochemistry kinetics of SAM are based on the mixture of electroactive molecules with saturated

alkanethiols so that the electroactive moieties can be separated much from each other. To form the mixed monolayers, one important factor is that the alkyl chain of the saturated alkanethiol molecules should not be longer than that of the electroactive molecules, or the redox potential shifts remarkably due to the potential drop within the monolayer [11–15]. Before examining the surfactant effect, knowing the character of the mixed monolayer without surfactant is of great importance. Fig. 1 shows the typical cyclic voltammograms (CVs) of the mixed monolayers of HSC<sub>11</sub>Fc and HSC<sub>8</sub> in 0.1 M HClO<sub>4</sub> electrolyte. The total concentration of the mixed solution is 1.0 mM and the mole fractions ( $\chi_{Fc}$ ) of HSC<sub>11</sub>Fc in solution are 0.9, 0.6, 0.3 and 0.1, respectively. For the high mole fraction,  $\chi_{Fc}=0.9$ , the CV shows a shoulder peak, indicating that some kinds of repulsive interactions exist between the electroactive moieties in the monolayer [49]. For low values of  $\chi_{Fc}$ , one pair of redox peaks is observed with the apparent formal potential,  $E^{\circ'}$ , (determined from the mean of the oxidation and reduction peak potentials) about 225 mV, and the separation between them ( $\Delta E_{opp}$ ) is only several mV, indicating that the electron transfer process is rather rapid and reversible. Inset in Fig. 1 is the relationship between peak currents and scan rate for the anodic process ( $\chi_{Fc}=0.6$ ). The peak currents exhibit a linear dependence on the scan rate in the range from 0.01 to 1.0 Vs<sup>-1</sup>, indicating that the electrode process is characteristic of surface-confined electroactive layer [5].

Fig. 2 is the relationship between the surface coverage and the mole fraction  $\chi_{Fc}$  of HSC<sub>11</sub>Fc in the mixed ethanol solution. The surface coverage rises slowly at low  $\chi_{Fc}$  and, then, an abrupt increase follows when  $\chi_{Fc}$  is close to 1. For the strongly bound two adsorbates, a simple linear relationship between the surface coverage and  $\chi_{Fc}$  would be expected [6,11]. Therefore, the trend in Fig. 2 can be explained as different solubilities of the two components or different bonding sites existing at the gold substrate surface, either of which will affect the adsorption-desorption equilibria for the two components.

In an ideal case when no interaction between the redox centers occurs, the full-width at half-maximum of the anodic voltammetric wave ( $\Delta E_{fwhm}$ ), is equal to 3.53RT/nF, that is 91.3 mV at 27 °C for one-electron reversible process [49]. However,  $\Delta E_{fwhm}$  of the

Table 2

Literature results of the mixed monolayers of HSRFc and thiols on gold electrode

Mixed SAM	$\chi_{Fc}$	$\Delta E_{fwhm}/mV$	$E^{\circ'}/mV$	$\Gamma/10^{-10} \text{ mol cm}^{-2}$	Reference
HSC <sub>16</sub> (CO <sub>2</sub> )Fc/HSC <sub>16</sub>	0.1	95	820 vs Ag		[6]
HSC <sub>11</sub> (CO <sub>2</sub> )Fc/HSC <sub>10</sub>	0.25	90	505 vs Ag/AgCl	1.6	[7]
HSC <sub>6</sub> Fc/HSC <sub>6</sub>	0.05		200 vs Ag/AgCl	0.29	[11]
HSC <sub>6</sub> Fc/HSC <sub>6</sub>	0.75	<sup>a</sup>	240 vs Ag/AgCl	2.9	[11]
HSC <sub>7</sub> (NH)(CO)Fc/HSC <sub>6</sub>		130	520 vs Ag/AgCl	0.05–0.1	[15]
HSC <sub>11</sub> (CO <sub>2</sub> )Fc/HSC <sub>10</sub>	0.5	145	540 vs Ag/AgCl	0.15	[22]
HSC <sub>2</sub> (CO)(NH)C <sub>11</sub> (CO <sub>2</sub> )Fc /HSC <sub>16</sub>	0.25	135	461 vs CE(3 M NaCl)	0.42	[33]
HSC <sub>2</sub> (CO)(NH)C <sub>11</sub> (CO <sub>2</sub> )Fc /HSC <sub>16</sub>	0.9	230	502 vs CE(3 M NaCl)	3.8	[33]
HSC <sub>8</sub> (CO <sub>2</sub> )Fc/MOT	0.1	96	620 vs Ag/AgCl		[46]
HSC <sub>16</sub> Fc/HSC <sub>11</sub> COOH	0.1	129	–220 vs MSE	0.86	[34]
HSC <sub>16</sub> Fc/HSC <sub>11</sub> COOH	0.4	<sup>a</sup>	–19 vs MSE	5.8	[34]
HSC <sub>6</sub> Fc/HSC <sub>6</sub> COOH	0.25	<sup>a</sup>	–300 vs MSE	0.9	[35]
HSC <sub>12</sub> Fc/HSC <sub>10</sub>	0.1	100	190 vs Ag/AgCl	1.4	[37]
HSC <sub>12</sub> Fc/HSC <sub>10</sub>	0.6	83	250 vs Ag/AgCl	4.2	[37]

<sup>a</sup>There are two peaks too close to define the full-width at half-maximum of each voltammetric wave precisely.

mixed monolayer (Table 1) is somewhat larger than the ideal value, and larger when  $\chi_{\text{Fc}}$  is higher, indicating that there is interaction between the redox Fc moieties even for low  $\chi_{\text{Fc}}$ . These observations are similar to those reported previously (Table 2), for example, ideal electrochemical behaviors of ferrocene-terminated alkanethiol are only described in literature for very low mole fraction ferrocene-terminated alkanethiol in mixed monolayer, mostly the redox peaks are nonideal especially when the mole fraction is high. The slightly larger  $\Delta E_{\text{fwhm}}$  infers that some HSC<sub>11</sub>Fc molecules are clustered and not isolated by HSC<sub>8</sub>.

### 3.2. Influence of surfactant in mixed monolayer

To compare the electrochemical behavior of HSC<sub>11</sub>Fc SAMs in different microenvironments, the mixed monolayer is examined with adsorption of ionic surfactant solution. Fig. 3 is the CVs of the mixed monolayer of HSC<sub>11</sub>Fc and HSC<sub>8</sub> ( $\chi_{\text{Fc}}=0.6$ ) before and after adsorption of anionic surfactant SDBS (Fig. 3a) and cationic surfactant CTAB (Fig. 3b). After aforementioned treatment, a shoulder peak (peak II) appears near to original peak I for both ion surfactants, proving that the corresponding Fc moieties are located in a different microenvironment. For the scan

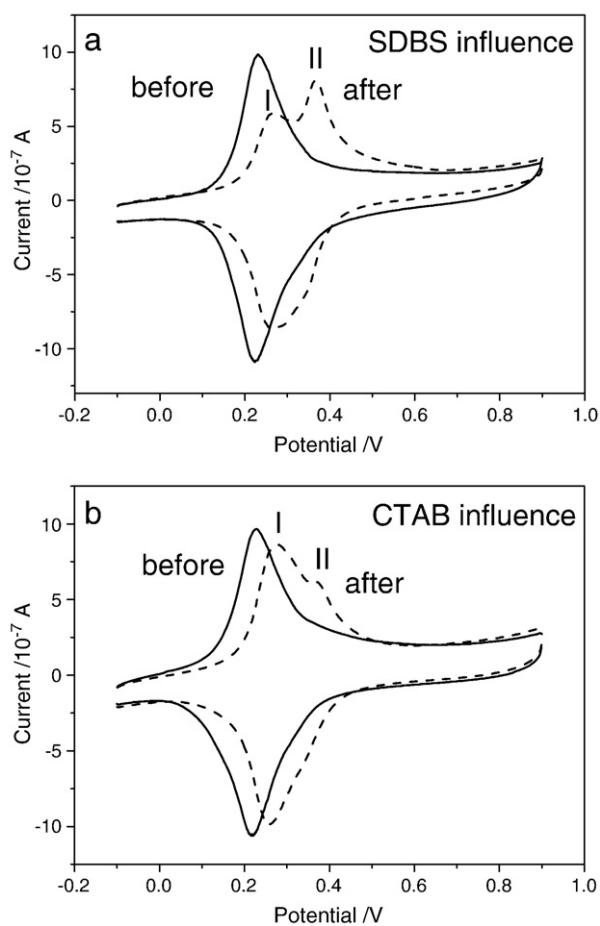


Fig. 3. Cyclic voltammograms of the mixed monolayer ( $\chi_{\text{Fc}}=0.6$ ) before (solid curve) and after (dashed curve) immersed in 0.05 M anionic surfactant SDBS (a) and 0.05 M cationic surfactant CTAB (b). Electrolyte: 0.1 M HClO<sub>4</sub>. Scan rate: 0.1 V s<sup>-1</sup>. Reference electrode: SCE, counter electrode: Pt.

Table 3

The peak II position and the ratio of peak height ratio II/I and peak area ratio II/I<sup>a</sup> for different surfactant concentrations

Surfactant concentration/M	SDBS			CTAB		
	Peak II position / V	Peak height ratio II/I	Peak area ratio II/I	Peak II position / V	Peak height ratio II/I	Peak area ratio II/I
0.002	0.370	0.86	1.12	0.365	0.56	0.47
0.01	0.368	1.46	1.35	0.365	0.55	0.51
0.05	0.368	1.41	1.31	0.370	0.64	0.61

<sup>a</sup>Data of peak I and peak II are derived from peak fitting using Gaussian function.

rate ranging between 0.01 and 1.0 Vs<sup>-1</sup>, the separation and the current ratio between peak I and peak II is almost constant. However, faster potential scan drives peak II farther separated from peak I with current ratio increased.

To find out the reason for peak II, concentration effect is studied. Changing the surfactant concentration (0.002, 0.01 and 0.05 M), peak II appears at almost the same position in each surfactant/mixed monolayer system. We also note when the surfactant concentration becomes higher, peak II becomes higher and larger compared with peak I for both ionic surfactant (Table 3). On the basis of these results, the appearance of peak II looks like coming from the effect of the ionic surfactant. However, for SDBS and CTAB, the current ratio of peak I/II is different, which may be related to their different ion radius and charge carried.

In former experiments, the electrolyte contains no surfactant molecules, and the adsorbed surfactant molecules could be desorbed back more or less. To further study the surfactant effect, we compare the electrochemistry of the surfactant-treated HSC<sub>11</sub>Fc SAMs in the electrolyte with/without surfactants. We do not observe any change in the CV plot when gradually increase the surfactant concentration until 0.5 mM, indicating that surfactant ad-desorption balance does not have much effect on the electrochemical behavior. However, when the surfactant concentration in electrolyte is 5 mM or higher, the redox potential is changed since the surfactant involved in the redox process of Fc as counterion as reported previously [46].

The dependence of the reduction (or oxidation) peak's position on the potential scan rate can be used to characterize the electron-transfer rate constant  $k_{\text{et}}$  and from the trumpet-like plots at high scan rate we can get the reorganization energy  $\lambda$ . Both  $k_{\text{et}}$  and  $\lambda$  can give us the information of the electron transfer process of the system studied. Fig. 4 shows plots of peak I potential (the upper and lower data are for the oxidation and reduction potentials, respectively) versus the natural logarithm of the potential scan rate for the dilute HSC<sub>11</sub>Fc monolayer before and after the ionic surfactant influence, along with the best fit to the Marcus theory [50,51]:

$$k_{\text{et}} = \frac{2\pi}{\hbar} |H_{\text{AD}}|^2 \frac{1}{\sqrt{4\pi\lambda k_{\text{B}}T}} \exp \left[ -\frac{(\lambda + (\varepsilon_{\text{F}} - \varepsilon) + e\eta)^2}{4\lambda k_{\text{B}}T} \right] \quad (1)$$

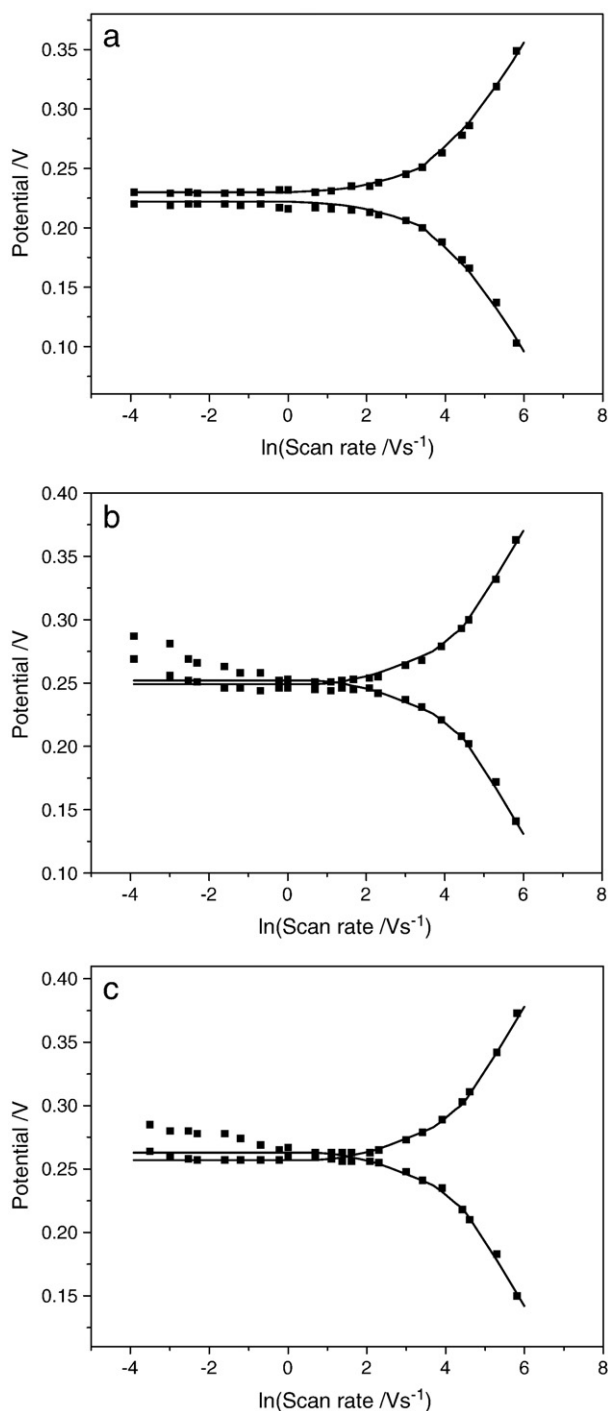


Fig. 4. The dependence of the peak potential on the natural logarithm of scan rate for CVs in Fig. 3. (a) for the mixed monolayer ( $\chi_{\text{Fc}}=0.6$ ) (b) for the influence of anionic surfactant SDBS (c) for the influence of cationic surfactant CTAB. The solid lines are the best fit to the data points using the Marcus theory described in the text.

where  $H_{\text{AD}}$  is the electronic coupling matrix element between electronic states in the electrode and the redox-active molecule,  $\lambda$  is the reorganization energy,  $\varepsilon_{\text{F}}$  is the Fermi level of the electrode,  $\varepsilon$  is the energy of a given state in the electrode, and  $\eta$  is the overpotential. We use self-written programs with Matlab on computers according to Eq. (1) to fit the experimental data.

For the dilute  $\text{HSC}_{11}\text{Fc}$  monolayer, the simulation gives the standard rate constants  $k_{\text{et}}$  and reorganization energy  $\lambda$  of  $650 \text{ s}^{-1}$  and  $0.85 \text{ eV}$ , respectively. These values are very close to those reported for normal alkanethiol monolayers with ferrocene redox centers [40,6,51]. After the ionic surfactant influence, the midpoint potential ( $E_{\text{a,c}}=(E_{\text{a}}+E_{\text{c}})/2$ ) shifts positively, deviating from Marcus fit, just as observed in Fig. 3. Neglecting the data at very low scan rates, we performed the simulation and got an identical  $k_{\text{et}}$ , but an increased  $\lambda$  ( $1.0 \text{ eV}$ ). The reorganization energies might be treated as a diagnostic parameter for the change of the local microenvironment of the ferrocene moieties [52–55]. The increased reorganization energy indicates that the microenvironment of electroactive Fc moieties became more polar.

Under the influence of the surfactants, one notable character is the positive shift of the peak I both in Figs. 3 and 4, especially for low scan rate. It might be the results of both counterion effect and neighboring ionic group effects. On the one side, the adsorbed surfactant adlayer may impede the counterion motion toward the redox sites at some degree, on the other side, the neighboring ionic groups increase the difficulty of ferrocenium ion from ferrocene. Creager and Nuzzo et al. also showed the positive shift of the ferrocene redox peaks when added ethanol and phospholipid surfactants, respectively [56,45]. However, when the scan rate is fast enough, the influence of microenvironment is not obvious.

### 3.3. Self-assembly dynamic study and influence of surfactant in pure $\text{HSC}_{11}\text{Fc}$ monolayer

Study on the formation of pure electroactive monolayer is of essential importance for the application in the high-density devices, and it is easy to interpret voltammograms and extract kinetic information. Fig. 5 gives the CV plots for  $10 \mu\text{M}$   $\text{HSC}_{11}\text{Fc}$  at different self-assembly time. We could find that at the initial stage, when the surface coverage is quite low, only one pair of redox peaks appears, very similar to the peak position of diluted ferrocene moieties as shown in Fig. 1. Then, as the surface coverage gradually increases, peak I positively shifts and peak II

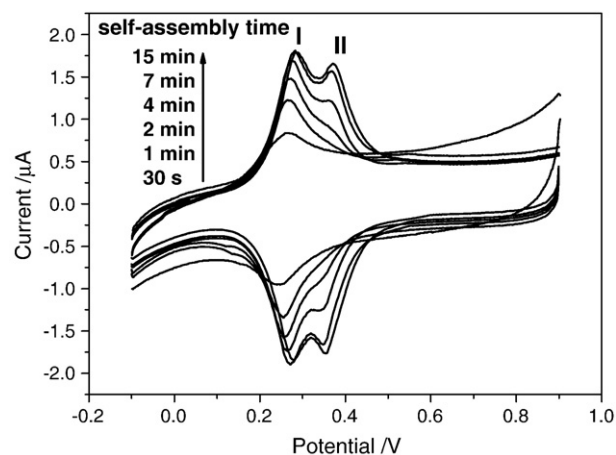


Fig. 5. Cyclic voltammograms of  $\text{HSC}_{11}\text{Fc}$ -SAM on gold with different self-assembly time: 30 s, 1 min, 2 min, 4 min, 7 min and 15 min. The concentration of deposition solution is  $10 \mu\text{M}$   $\text{HSC}_{11}\text{Fc}$  ethanol solution. Electrolyte:  $0.1 \text{ M}$   $\text{HClO}_4$ . Scan rate:  $0.1 \text{ V s}^{-1}$ . Reference electrode: SCE, counter electrode: Pt.

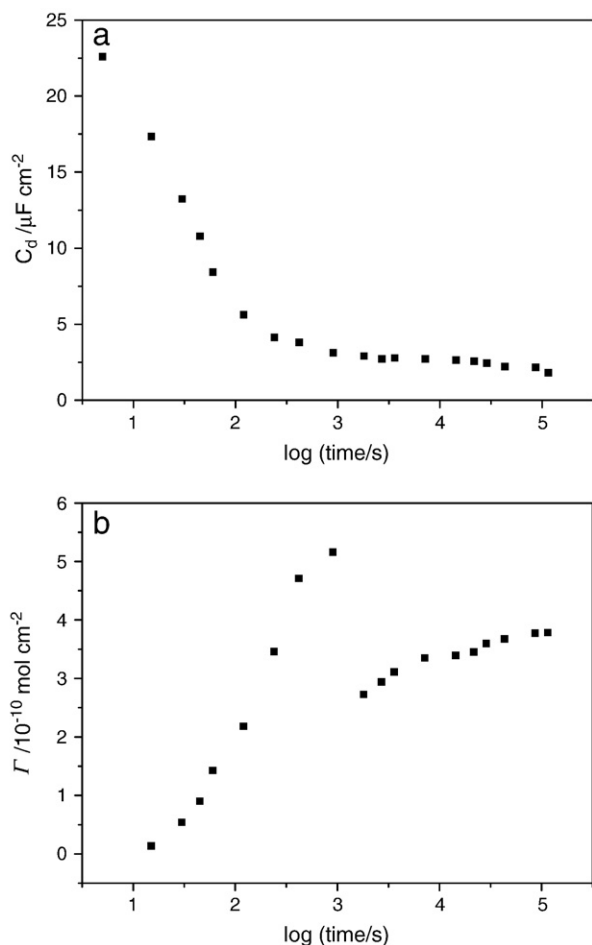


Fig. 6. Variations of (a) differential capacitance; and (b) surface coverage of HSC<sub>11</sub>Fc-SAM on gold versus the self-assembly time in 10  $\mu\text{M}$  ethanol solution. Electrolyte: 0.1 M HClO<sub>4</sub>. Scan rate: 0.1 V s<sup>-1</sup>. Reference electrode: SCE, counter electrode: Pt.

appears. Two peaks imply two different microenvironments [57]. Peak I is for dilute Fc oxidation which is less influenced by intermolecular interaction. As for the origin of peak II, they appear when the density is high or ionic surfactant is presented. It is believed that the polar microenvironment plays an important role in peak II. When some Fc moieties are oxidized to Fc<sup>+</sup>, they generate a positive ionic microenvironment for the Fc moiety in close proximity, which increases the difficulty of the further oxidation, causing peak II and shifting peak I.

Fig. 6 is the change of capacitance and surface coverage with the self-assembly time. The differential capacitance ( $C_d$ ) of a monolayer is easily estimated from the capacitive charging current divided by the scan rate and electrode surface area. Fig. 6a shows  $C_d$  dramatically decreases in the early self-assembly stage and then gradually reaches its final value. The decrease in  $C_d$  can be explained by the fact that the differential capacitance is inversely proportional to the increasing monolayer thickness, which is on the basis of Helmholtz theory. The change of surface coverage (Fig. 6b) is quite different from those of alkanethiol self-assembly reported previously [58,59]. There is a sudden steep dropping at about 15 min. inferring some change of preferred molecular orientation process. Usually, the self-assembly process

of alkanethiol is composed of two steps [58,60]. The first is a rapid physical adsorption, in which the self-assembled molecule may lay on the gold surface. Due to the stronger intermolecular interaction of HSC<sub>11</sub>Fc than other small molecules, multilayer is most likely formed in this step. The next step is a reorientation of the laying molecules. After this step a small part of the physically adsorbed molecules may stand up with only the head group attached onto the surface, losing the extra physically adsorbed molecules. Therefore, a decrease of the apparent surface coverage was found in the experiment.

Fig. 7 shows the CVs of the pure HSC<sub>11</sub>Fc monolayer before and after the adsorption of anionic surfactant SDBS (Fig. 7a) and cationic surfactant CTAB (Fig. 7b). The mean surface coverage ( $\Gamma$ ) of HSC<sub>11</sub>Fc is about  $4.3 \times 10^{-10} \text{ mol cm}^{-2}$ , consistent well with the full coverage  $4.5 \times 10^{-10} \text{ mol cm}^{-2}$  expected from the hexagonal closed-packing of 6.6 Å diameter spheres for the ferrocene group [7]. Without the treatment with the surfactant, the CV plots show two broad waves with  $\Delta E_{\text{fwhm}}$  much larger than the value of 91.3 mV. Similar results have been also reported by other research groups for such pure ferrocene-

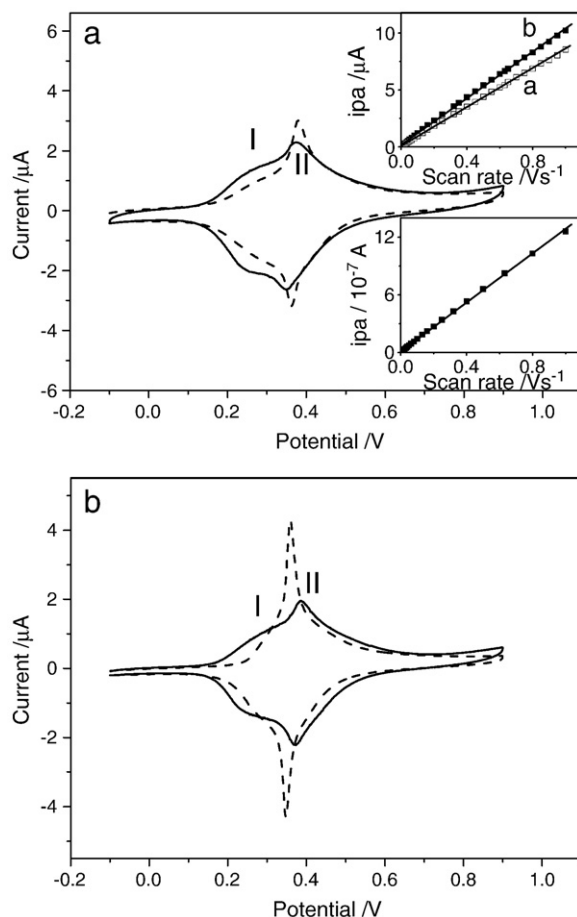


Fig. 7. Cyclic voltammograms of the pure HSC<sub>11</sub>Fc monolayer (adsorption solution: 1 mM) before (solid curve) and after (dash curve) immersed in 0.05 M anionic surfactant SDBS (a) and 0.05 M cationic surfactant CTAB (b). Upper inset in Fig. 3a is linear relations of peak currents versus scan rates for the first anodic process (I) and for the second anodic process (II). Lower inset is the linear relation of peak currents and scan rates for the anodic process of the HSC<sub>11</sub>Fc and SDBS system. Electrolyte: 0.1 M HClO<sub>4</sub>. Scan rate: 0.1 V s<sup>-1</sup>. Reference electrode: SCE, counter electrode: Pt.

terminated monolayers[9,18,20,21,24–26,61,62]. After the surfactant treatment, the adsorbed surfactant ions may form the specific ionic microenvironment prior to the oxidation, therefore, peak I is much decreased and peak II increased.

We also noted another important feature of CVs. After the influence of surfactant, peak II is so narrow and sharp with  $\Delta E_{\text{fwhm}}$  less than 91.3 mV. Such a sharp peak reflects the attraction force, according to the model proposed by Laviron [28,63]. For anionic sulfonic ions, there is attraction force between the anionic surfactant ion and the  $\text{Fc}^+$ . As for the cationic ammonium groups, considering the charge balance and counterion effect, those anions, such as  $\text{Br}^-$  and  $\text{ClO}_4^-$ , may form another free adlayer attached to the ammonium groups [64,65], therefore, attraction between the adlayer anionic and  $\text{Fc}^+$  is observed.

#### 4. Conclusions

The present experimental work presents that the polar microenvironment caused by either ionic surfactants or charged redox centers plays an important role in the electrochemical behavior of the electroactive SAMs. The ionic surfactants are demonstrated to be able to adjust the polar microenvironment as evidenced by the variation of reorganization energy. When  $\text{HSC}_{11}\text{Fc}$  of low density mixed with other inert monolayers is treated with surfactants, the local ionic environment causes a pair of shoulder peaks. On the other hand, in a pure  $\text{HSC}_{11}\text{Fc}$  monolayer, the shoulder peak emerges as a result of positively charged microenvironment. Further treatment with the surfactants may lead to much enhanced shoulder peak corresponding to the modified local microenvironment.

#### Acknowledgements

This project is supported by the National Nature Science Foundation of China (No.20503012 and No.20435010) and Open Foundation of State Key Laboratory of Bioelectronics of Southeast University.

#### References

- [1] R.G. Nuzzo, D.L. Allara, J. Am. Chem. Soc. 105 (1983) 4481.
- [2] A. Ulman, An Introduction to Ultrathin Organic Films: From Langmuir-Blodgett to Self-Assembly, Academic Press, San Diego, CA, 1991.
- [3] J.C. Love, L.A. Estroff, J.K. Kriebel, R.G. Nuzzo, G.M. Whitesides, Chem. Rev. 105 (2005) 1103.
- [4] A. Ulman, Chem. Rev. 96 (1996) 1533.
- [5] H.O. Finklea, in: A.J. Bard, I. Rubinstein (Eds.), Electroanalytical Chemistry, vol. 19, Marcel Dekker, New York, 1996, p. 109.
- [6] C.E.D. Chidsey, Science 251 (1991) 919.
- [7] C.E.D. Chidsey, C.R. Bertozzi, T.M. Putvinski, A.M. Muijsce, J. Am. Chem. Soc. 112 (1990) 4301.
- [8] J.P. Collman, N.K. Devaraj, C.E.D. Chidsey, Langmuir 20 (2004) 1051.
- [9] K. Uosaki, Y. Sato, H. Kita, Langmuir 7 (1991) 1510.
- [10] K. Uosaki, Y. Sato, H. Kita, Electrochim. Acta 36 (1991) 1799.
- [11] G.K. Rowe, S.E. Creager, Langmuir 7 (1991) 2307.
- [12] S.E. Creager, G.K. Rowe, Anal. Chim. Acta 246 (1991) 233.
- [13] G.K. Rowe, S.E. Creager, J. Phys. Chem. 98 (1994) 5500.
- [14] S.E. Creager, G.K. Rowe, Langmuir 10 (1994) 1186.
- [15] S.E. Creager, G.K. Rowe, J. Electroanal. Chem. 420 (1997) 291.
- [16] J.J. Sumner, S.E. Creager, J. Phys. Chem. B 105 (2001) 8739.
- [17] J.A.M. Sondag-Huethorst, L.G.J. Fokkink, Langmuir 10 (1994) 4380.
- [18] N.L. Abbott, G.M. Whitesides, Langmuir 10 (1994) 1493.
- [19] D.M. Collard, M.A. Fox, Langmuir 7 (1991) 1192.
- [20] M.M. Walczak, D.D. Popenoe, R.S. Deinhammer, B.D. Lamp, C. Chung, M.D. Porter, Langmuir 7 (1991) 2687.
- [21] M. Péter, R.G.H. Lammertink, M.A. Hempenius, G.J. Vancso, Langmuir 21 (2005) 5115.
- [22] R. Voicu, T.H. Ellis, H. Ju, D. Leech, Langmuir 15 (1999) 8170.
- [23] T. Kawaguchi, K. Tada, K. Shimazu, J. Electroanal. Chem. 543 (2003) 41.
- [24] S. Ye, Y. Sato, K. Uosaki, Langmuir 13 (1997) 3157.
- [25] K. Seo, I.C. Jeon, D.J. Yoo, Langmuir 20 (2004) 4147.
- [26] F. Quist, V. Tabard-Cossa, A. Badia, J. Phys. Chem. B 107 (2003) 10691.
- [27] T.T.-T. Li, M.J. Weaver, J. Am. Chem. Soc. 106 (1984) 6107.
- [28] E. Laviron, J. Electroanal. Chem. 52 (1974) 395.
- [29] J.J. Sumner, K.S. Weber, L.A. Hockett, S.E. Creager, J. Phys. Chem. B 104 (2000) 7449.
- [30] J.J. Sumner, S.E. Creager, J. Am. Chem. Soc. 122 (2000) 11914.
- [31] C.P. Smith, H.S. White, Anal. Chem. 64 (1992) 2398.
- [32] W.R. Fawcett, J. Electroanal. Chem. 378 (1994) 117.
- [33] R.C. Chambers, C.E. Inman, J.E. Hutchison, Langmuir 21 (2005) 4615.
- [34] T. Auletta, F.C.J.M. van Veggel, D.N. Reinhoudt, Langmuir 18 (2002) 1288.
- [35] M.W.J. Beulen, F.C.J.M. van Veggel, D.N. Reinhoudt, Chem. Commun. (1999) 503.
- [36] R.C. Sabapathy, S. Bhattacharyya, M.C. Leavy, W.E. Cleland Jr., C.L. Hussey, Langmuir 14 (1998) 124.
- [37] L.Y.S. Lee, T.C. Sutherland, S. Rucareanu, R.B. Lennox, Langmuir 22 (2006) 4438.
- [38] J.J. Calvente, R. Andreu, M. Molero, G. López-Pérez, M. Dominguez, J. Phys. Chem. B 105 (2001) 9557.
- [39] J.T. Hupp, M.J. Weaver, J. Electrochem. Soc. 131 (1984) 619.
- [40] H. Ju, D. Leech, Phys. Chem. Chem. Phys. 1 (1999) 1549.
- [41] A.W. Adamson, Physical Chemistry of Surfaces, fifth ed., John Wiley and Sons, New York, 1990.
- [42] E. Sackmann, Science 271 (1996) 43.
- [43] A.L. Plant, Langmuir 15 (1999) 5128.
- [44] A.L. Plant, Langmuir 9 (1993) 2764.
- [45] M. Twardowski, R.G. Nuzzo, Langmuir 19 (2003) 9781.
- [46] Z. Peng, X. Qu, S. Dong, J. Electroanal. Chem. 563 (2004) 291.
- [47] H. Angerstein-Kozłowska, in: E. Yeager, J.O'M. Bockris, B.E. Conway, S. Sarangapani (Eds.), Comprehensive Treatise of Electrochemistry, vol. 9, Plenum Press, New York, 1984, ch. 9.
- [48] B.E. Conway, W.B.A. Sharp, H. Angerstein-Kozłowska, E.E. Criddle, Anal. Chem. 45 (1973) 1321.
- [49] A.J. Bard, L.R. Faulkner, Electrochemical Methods: Fundamentals and Applications, Second ed., John Wiley and Sons, New York, 2001.
- [50] R.A. Marcus, J. Chem. Phys. 43 (1965) 679.
- [51] K. Weber, S.E. Creager, Anal. Chem. 66 (1994) 3164.
- [52] K. Slowinski, K.U. Slowinska, M. Majda, J. Phys. Chem. 103 (1999) 8544.
- [53] S. Sek, A. Misicka, R. Bilewicz, J. Am. Chem. Soc. 104 (2000) 5399.
- [54] Z. Peng, S. Dong, Langmuir 17 (2001) 4904.
- [55] Z. Peng, J. Tang, X. Han, E. Wang, S. Dong, Langmuir 18 (2002) 4834.
- [56] S.E. Creager, G.K. Rowe, Langmuir 9 (1993) 2330.
- [57] R. Rulkens, A.J. Lough, I. Manners, S.R. Lovelace, C. Grant, W.E. Geiger, J. Am. Chem. Soc. 118 (1996) 12683.
- [58] C.D. Bain, E.B. Troughton, Yu.-T. Tao, J. Evall, G.M. Whitesides, R.G. Nuzzo, J. Am. Chem. Soc. 111 (1989) 321.
- [59] J.D. Tirado, D. Acevedo, R.L. Bretz, H.D. Abruña, Langmuir 10 (1994) 1971.
- [60] R. Georgiadis, K.P. Peterlinz, A.W. Peterson, J. Am. Chem. Soc. 122 (2000) 3166.
- [61] A. Anne, J. Moiroux, Macromolecules 32 (1999) 5829.
- [62] T. Fushimi, A. Oda, H. Ohkita, S. Ito, Thin Solid Films 484 (2005) 318.
- [63] E. Laviron, in: A.J. Bard (Ed.), Electroanalytical Chemistry, vol. 12, Marcel Dekker, New York, 1982, pp. 53–157.
- [64] R. Zana, Langmuir 12 (1996) 1208.
- [65] Y. Ono, H. Kawasaki, M. Annaka, H. Maeda, J. Colloid Interface Sci. 287 (2005) 685.